^{1}H NMR Studies of Tris(phenanthroline) Metal Complexes Bound to Oligonucleotides: Structural Characterizations via Selective Paramagnetic Relaxation†

Jill P. Rehmann and Jacqueline K. Barton*,‡
Department of Chemistry, Columbia University, New York, New York 10027
Received June 30, 1989; Revised Manuscript Received October 19, 1989

ABSTRACT: The selective paramagnetic relaxation of oligonucleotide protons of $d(GTGCAC)_2$ by Δ- and Λ-$Ni(phen)_3^{3+}$ and Δ- and Λ-$Cr(phen)_3^{3+}$ has been examined to obtain some structural insight into the noncovalent binding of tris(phenanthroline) metal complexes to DNA. The experiments demonstrate that the relative rate of relaxation of different oligonucleotide protons by the paramagnetic metal complex varies with the chirality of the metal complex and, to a lesser extent, the metal charge. The proton most efficiently relaxed in all cases is the adenosine AH2, which is situated in the minor groove of the oligonucleotide helix. For both Λ-$Ni(phen)_3^{2+}$ and Λ-$Cr(phen)_3^{3+}$, the order of relaxation rates varies as AH2 ≫ AH8 > G3H8 = TMe = C4H5. For Δ-$Ni(phen)_3^{2+}$ it varies as AH2 > G3H8 > AH8 > TMe = C4H5 and for Δ-$Cr(phen)_3^{3+}$ as AH2 > TMe = G3H8 = AH8 > C4H5. Distances between the metal center and oligonucleotide protons were calculated on the basis of the relaxation data, and these distances were used to generate a set of models to describe the interactions of the rigid metal complex with the helix. For Λ-isomers, the data are consistent with a predominant surface-bound association in the minor groove of the DNA helix. The results for Δ-isomers correlate better with models that incorporate also a major groove intercalative mode. Despite the absence of hydrogen-bonding groups in the metal complex, the surface-bound model of the phenanthroline complex in the minor groove of DNA resembles the noncovalent association seen with other DNA groove binding molecules.

Tris(1,10-phenanthroline) metal complexes bind enantioselectively to DNA (Barton, 1986). Photophysical studies have shown that the complexes bind to DNA through two distinct binding modes, and each has an associated enantiomeric preference. One mode, attributed to intercalation, favors the Δ-isomer, while the surface-bound mode favors the Λ-isomer (Barton et al., 1984, 1986; Kumar et al., 1985). NMR studies of tris(phenanthroline) complexes of ruthenium(II), rhodium(III), and cobalt(III) (Rehmann & Barton, 1990) bound to oligonucleotides have yielded some additional features of each binding mode. In particular, these studies have allowed a greater elucidation of the surface-binding interaction of the metal complexes with nucleic acids, the binding mode more difficult to characterize by photophysical techniques.

In this companion study, we have taken advantage of the enhancement of oligonucleotide proton relaxation generated by a paramagnetic ion, which is inversely proportional to the inverse sixth power of the distance between the proton and the paramagnetic center, to examine structural characteristics associated with these binding interactions. Transfer NOE studies could not be performed between the metal complexes and oligonucleotide owing likely to the low affinity of the complexes for DNA, the complexity of the binding interactions, and the fast exchange of the phenanthrolines between structurally inequivalent positions in the bound complex. Application of the paramagnetic analogues of the tris(phenanthroline) complexes therefore has permitted some structural information, particularly regarding the groove locations of the bound complex, to be obtained on this system via NMR. Substitution of paramagnetic transition metal ions for diamagnetic ions in the tris(phenanthroline) complex should cause little structural perturbation in the overall complex compared to the parent diamagnetic complex, and hence, recognition characteristics of the di- and trivalent paramagnetic complexes ought to parallel well the binding features of their diamagnetic analogues. The fact that the paramagnetic ions employed are coordinatively saturated and hence would not coordinate directly to the DNA also precludes many of the complications often encountered with this method owing to uncertainities as to the relative contributions of scalar and dipolar relaxation mechanisms.

NMR studies of tris(phenanthroline) complexes of nickel(II) and chromium(III) bound to duplex oligonucleotides were therefore undertaken. Enantiomers of the paramagnetic $Ni(phen)_3^{2+}$ and $Cr(phen)_3^{3+}$ ions bound to the oligonucleotide $d(GTGCAC)_2$ are found to increase the relaxation rates of specific nucleic acid protons. The relative order in which the protons are affected by the complex has been used to construct a structural model for the orientation of the paramagnetic complex with respect to the DNA helix. The analysis is consistent with a model where surface binding by the Λ-enantiomer occurs in the minor groove of the helix.

Experimental Procedures

Materials

Synthesis of Tris(1,10-phenanthroline)nickel(II) Chloride. $[Ni(phen)_3]Cl_2$ was synthesized as described previously (Kauffman & Takahashi, 1966). Extinction coefficients: $\epsilon_{267} = 8.43 \times 10^4$ M^{-1} cm^{-1}; $\epsilon_{522} = 10.1$ M^{-1} cm^{-1}; $\epsilon_{784} = 6.1$ M^{-1} cm^{-1}. Anal. Calcd for $[Ni(C_{12}H_8N_2)_3]Cl_2 \cdot 2.5H_2O$: C, 60.46; H, 4.06; N, 11.76; Ni, 8.22. Found: C, 60.48; H, 4.16; N, 11.74; Ni, 8.16.

† This work was supported by NIH Grant GM33309.
* Author to whom correspondence and reprint requests should be addressed.
‡ Present address: Division of Chemistry and Chemical Engineering, California Institute of Technology, Pasadena, CA 91125.

0006-2960/90/0429-1710$02.50/0 © 1990 American Chemical Society

Resolution of Tris(1,10-phenanthroline)nickel(II) Perchlorate. The enantiomers of $[Ni(phen)_3](ClO_4)_2$ were obtained by precipitation of a racemic solution with antimony *d*-tartrate (Kauffman & Takahashi, 1966). The Λ-enantiomer [100% Λ based on the literature value, $\Delta\epsilon_{273} = +636$ mol^{-1} cm^{-1}; lit. (Mason & Peart, 1973) $\Delta\epsilon_{273} = +550$ mol^{-1} cm^{-1}] was obtained from the precipitate, and the Δ-enantiomer (90% Δ,$\Delta\epsilon_{273} = -515$ mol^{-1} cm^{-1}) was isolated from the filtrate. Both enantiomers were used as the perchlorate salts.

Since $Ni(phen)_3^{2+}$ is known to racemize in solution (Davies & Dwyer, 1953), we evaluated the rate of this racemization for the purposes of our experiment. It was determined that ~80% enantiomeric purity remains after 24 h under the conditions of the NMR experiment. The possibility that the oligomer facilitates racemization cannot be precluded on the basis of this control, but the different results obtained with each enantiomer in this study suggest that the enantiomers remain largely intact in the presence of the oligonucleotide over the time scale of the experiment.

Synthesis of Chromium(II) Sulfate. Chromium(II) sulfate pentahydrate was prepared by dissolving chromium metal in concentrated H_2SO_4 under N_2, according to a previously published procedure (Hein & Herzog, 1965).

Synthesis of Tris(1,10-phenanthroline)chromium(III) Perchlorate. The following procedure was adapted from two previously published methods (Lee et al., 1966; Herzog, 1956). All solvents were thoroughly degassed prior to use and maintained under N_2. Chromous sulfate (1.62 g, 6.81 mmol) was dissolved in 60 mL of H_2O under N_2, to give a clear blue solution. 1,10-Phenanthroline monohydrate (6.74 g, 34.0 mmol) in 150 mL of absolute ethanol was added slowly to the chromous sulfate solution to generate a dark olive green-yellow solution. The solution was stirred under N_2 for 30 min. The solvents were removed under vacuum (overnight to ensure complete dryness) to give a black solid. The solid was resuspended in 150 mL of warm anhydrous ethanol, and the mixture was oxidized with I_2 (11.5 g, 4.54 mmol) in 50 mL of dry ethanol to generate a gold suspension. The mixture was stirred for 30 min and filtered. The gold solid was resuspended in 400 mL of warm H_2O and filtered to remove a small amount of red solid. Saturated $NaClO_4$ (30 mL) was added to the red filtrate to give fine golden yellow needles. Following two recrystallizations from H_2O (4 °C), 1.93 g (31% yield) of the desired product was obtained. Extinction coefficient: $\epsilon_{272} = 6.8 \times 10^4$ M^{-1} cm^{-1}. Low-resolution fast atom bombardment (FAB) mass spectrometry gave a molecular ion at 790 corresponding to $[Cr(phen)_3](ClO_4)_2^+$. Anal. Calcd for $[Cr(C_{12}H_8N_2)_3](ClO_4)_3 \cdot 2H_2O$: C, 46.7; H, 3.0; N, 9.1; Cr, 5.6. Found: C, 47.1; H, 3.0; N, 9.0; Cr, 5.7.

Resolution of Tris(1,10-phenanthroline)chromium(III) Perchlorate. Racemic $[Cr(phen)_3](ClO_4)_3$ was resolved by precipitation with $(+)_D$-$K_3[Co(cysu)_3]$ as described previously (Kane-Maguire & Hallock, 1979). The Λ-enantiomer [88% Λ, $\Delta\epsilon_{273} = +112$ mol^{-1} cm^{-1}; lit. (Mason & Peart, 1973) $\Delta\epsilon_{273} = +145$ mol^{-1} cm^{-1}] was obtained as the precipitate, and the Δ-enantiomer (88% Δ, $\Delta\epsilon_{273} = -112$ mol^{-1} cm^{-1}) was isolated from the filtrate. Both enantiomers were used as the perchlorate salts.

Synthesis and Purification of d(GTGCAC)$_2$. The oligodeoxyribonucleotide was synthesized by the phosphoramidite method and purified by HPLC on a μBondapac C_{18} Radial-Pac cartridge, chromatography on Sephadex G-25, and cation exchange to generate the sodium salt. Sequential proton resonance assignments were made by two-dimensional NOE spectroscopy according to the method described by Scheek et al. (1983). The samples were prepared by dissolving the oligonucleotide in 5 mM sodium phosphate buffer (pH 7.0) containing 15 mM NaCl and lyophilizing to dryness. D_2O (99.96% atom purity, Aldrich) was added to the sample and lyophilization was repeated three times. The final sample volume was 800 μL with a final nucleotide concentration of 19 mM. The $Cr(phen)_3^{3+}$ and $Ni(phen)_3^{2+}$ solutions were prepared in a similar manner.

Methods

NMR Measurements. ^{1}H NMR experiments were performed on Varian VXR-300 (300 MHz) and Varian VZR-400 (400 MHz) NMR spectrometers. Typical instrument settings for the 400-MHz were as follows: acquisition time, 0.994 s; sweep width, 4798 Hz; spectral size, 9536 data points, with 1-Hz line broadening. All experiments were carried out at 5 °C, and the spectra were referenced relative to TSP [3-(trimethylsilyl)-1-propanesulfonic acid] as an internal standard.

The proton spin–lattice relaxation times were measured by the inversion-recovery method using a 180–τ–90 pulse sequence and calculated by a nonlinear least-squares fit of measured peak height to

$$M_z(t) = M_0[1 - (1 - \cos\alpha)e^{-t/T}]$$

where M_0 is the equilibrium magnetization and α is the flip angle, which remains constant throughout the experiment.

Data Analysis. The effect that a paramagnetic species has on the longitudinal relaxation rate of a proton a distance r from the paramagnetic nucleus is described by the Solomon–Bloembergen equation (Solomon, 1955; Bloembergen & Morgan, 1961; Mildvan & Gupta, 1978):

$$\frac{1}{T_{1M}} = \frac{2}{15}\frac{S(S+1)\gamma^2 g^2\beta^2 f(\tau_c)}{r^6} + \frac{2}{3}\frac{S(S+1)A^2}{h^2}\frac{\tau_c}{1+\omega_S^2\tau_c^2} \quad (1)$$

$$f(\tau_c) = \frac{3\tau_c}{1+\omega_I^2\tau_c^2} + \frac{7\tau_c}{1+\omega_S^2\tau_c^2}$$

where S is the electron spin quantum number, γ is the gyromagnetic ratio of the proton, g is the electronic g factor, and β is the Bohr magneton. ω_I and ω_s (=657ω_I) are 2π times the Larmour frequencies of the nucleus and the electron, respectively. The second term of eq 1 accounts for the scalar or through-bond contribution to the relaxation rate. Since the tris(phenanthroline)metal complexes are already coordinatively saturated and bind the nucleic acid in a noncovalent manner, we have neglected the contributions of scalar coupling. The correlation time, τ_c, modulates the paramagnetic relaxation process and can be expressed as the sum of three components:

$$\frac{1}{\tau_c} = \frac{1}{\tau_r} + \frac{1}{\tau_s} + \frac{1}{\tau_m} \quad (2)$$

where τ_r is the rotational correlation time of the paramagnetic species bound to the macromolecule, τ_m is the mean lifetime of the bound complex, and τ_s is the electron spin-relaxation time. The relaxation rate enhancement of a given nucleus resulting from a paramagnetic species will depend on the concentration of the paramagnetic species as well as the lifetime of the bound complex:

$$\frac{1}{T_{1p}} = \frac{fq}{T_{1M} + \tau_m} \quad (3)$$

where f is the concentration ratio of the bound paramagnet to the total substrate concentration (given by the concentration

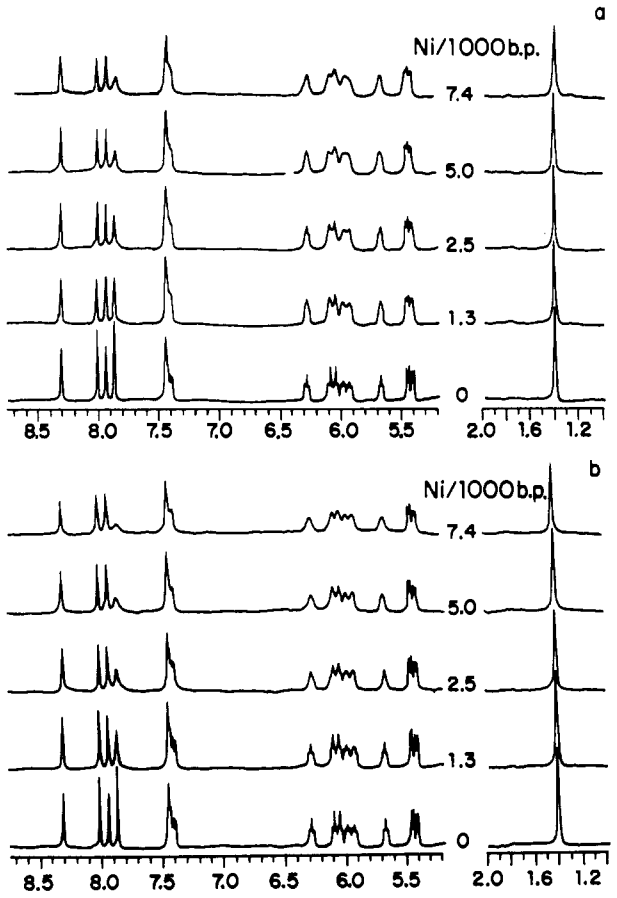

FIGURE 1: Effects of Δ- (a) and Λ- (b) $Ni(phen)_3^{2+}$ on the ^1H NMR spectrum of $d(GTGCAC)_2$ at 5 °C. The ratio of metal complex added to the oligonucleotide per base pair is indicated. Oligonucleotide proton assignments are as follows: AH8, 8.31; G1H8, 8.02; G3H8, 7.94; AH2, 7.87; pyrimidine H6, 7.44; AH1′, 6.28; C6H1′, 6.10; G1H1′, 6.05; TH1′, 5.98; G3H1′, 5.94; C4H1′, 5.68; CH5, 5.45; TMe, 1.40.

of duplex oligonucleotide) and q is the stoichiometry of the bound complex. The concentration-dependent relaxation rate enhancement due to the paramagnetic complex is

$$\frac{1}{T_{1p}} = \frac{1}{T_1} - \frac{1}{T_{10}} \quad (4)$$

where T_{10} represents the relaxation time of the proton measured in the absence of the paramagnetic complex and T_1 is the experimentally observed relaxation time of the proton in the complex. Values for all parameters used in these calculations, both those determined experimentally and those taken from the literature, are described in more detail under Distance Calculations.

Results and Discussion

^1H NMR Spectra of Paramagnetic Complexes Bound to $d(GTGCAC)_2$. Binding of paramagnetic $Ni(phen)_3^{2+}$ to $d(GTGCAC)_2$ results in broadening of the ^1H resonances in the NMR spectrum of the oligonucleotide. The effects of Δ- and Λ-$Ni(phen)_3^{2+}$ are shown in Figure 1. In the case of both enantiomers, increasing nickel(II) concentrations leads to the broadening of all ^1H resonances. Some preferential broadening of resonances associated with some protons on the oligonucleotide by the complexes can nonetheless be observed. The most extensively broadened resonance for both enantiomers corresponds to the H2 of adenine, centered at 7.88 ppm. In terms of differences in broadening between bound isomers, some differences are also evident. Most pronounced is the observation that the AH2 proton is broadened to a greater

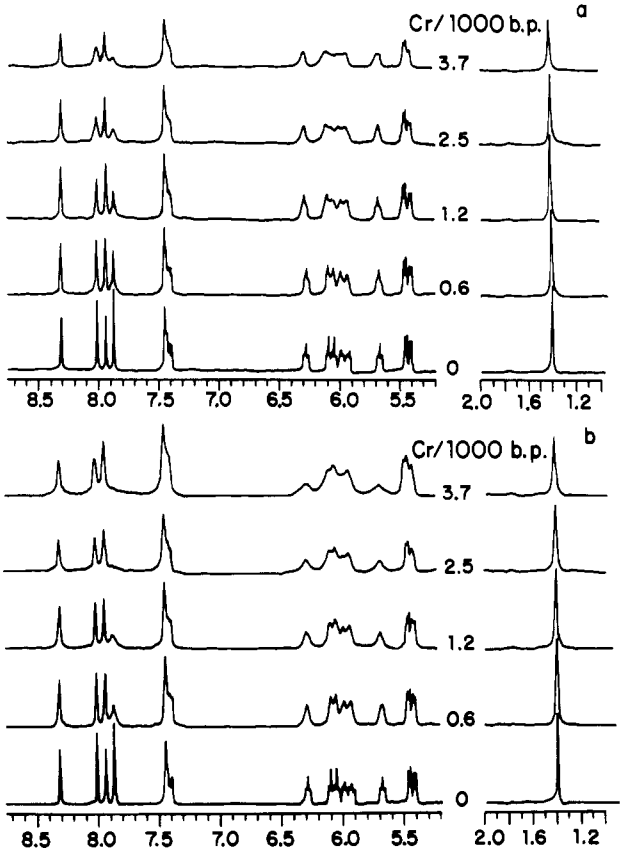

FIGURE 2: Effects of Δ- (a) and Λ- (b) $Cr(phen)_3^{3+}$ on the ^1H NMR spectrum of $d(GTGCAC)_2$ at 5 °C. Proton resonance assignments are as in Figure 1.

Table I: ^1H NMR Relaxation Parameters and Calculated Metal–Proton Distances for $(GTGCAC)_2$ in the Presence of $Ni(phen)_3^{2+}$

		Δ		Λ	
proton	δ (ppm)	$1/T_{1M}$ (s^{-1})	r (Å)[a]	$1/T_{1M}$ (s^{-1})	r (Å)
AH8	8.312	35.4	7.4 ± 0.3	72.9	6.7 ± 0.2
G3H8	7.940	61.7	6.8 ± 0.4	39.3	7.4 ± 0.2
AH2	7.871	441	4.9 ± 0.2	835	4.4 ± 0.2
TMe	1.398	22.5	8.0 ± 0.5	29.1	7.8 ± 0.2
C4H5	5.448	22.0	8.0 ± 0.9	37.8	7.4 ± 0.3
AH1′	6.284	123	6.0 ± 0.6	346	5.1 ± 0.2
C4H1′	5.676	119	6.1 ± 0.5	273	5.4 ± 0.2

[a] Uncertainties reported at the 95% confidence level.

extent when the oligonucleotide is titrated with the Λ-enantiomer compared to the Δ-isomer.

As can be seen in Figure 2, the effect of $Cr(phen)_3^{3+}$ on the spectrum of $d(GTGCAC)_2$ is similar to that of the nickel complex. Again, the AH2 proton undergoes the most extensive broadening upon addition of the metal complex, and the Λ-enantiomer is more efficient in broadening this resonance than is the Δ-isomer. In contrast to the nickel complex, $Cr(phen)_3^{3+}$ association also has a marked effect on the protons located at the end of the oligonucleotide, e.g., G1H8, C6H1′, and G1H1′ (centered at 8.02, 6.10, and 6.05 ppm, respectively). These resonances experience the most broadening when the Δ-enantiomer is bound to the oligonucleotide. The broadening observed at the ends of the oligonucleotide could reflect affinity of the complex for an altered DNA conformation since the ends of oligonucleotides are known to be more open or frayed in solution (Tran-Dinh et al., 1982).

Paramagnetic Relaxation Rate as a Function of Metal Concentration. Tables I and II indicate the values of $1/T_{1M}$

Table II: ^{1}H NMR Relaxation Parameters and Calculated Metal–Proton Distances for $(GTGCAC)_2$ in the Presence of $Cr(phen)_3^{3+}$

		Δ		Λ	
proton	δ (ppm)	$1/T_{1M}$ (s^{-1})	r (Å)[a]	$1/T_{1M}$ (s^{-1})	r (Å)
AH8	8.312	15.3	8.6 ± 0.3	32.1	7.9 ± 0.3
G3H8	7.940	17.1	8.4 ± 0.3	23.5	8.4 ± 0.4
AH2	7.871	89.9	6.4 ± 0.5	334	5.4 ± 0.3
TMe	1.398	19.9	8.2 ± 0.3	20.8	8.5 ± 0.2
C4H5	5.448	9.3	9.3 ± 0.3	17.0	8.8 ± 0.6
AH1′	6.284	31.0	7.6 ± 0.3	92.1	6.7 ± 0.2
C4H1′	5.676	25.5	7.9 ± 0.2	90.4	6.7 ± 0.2

[a] Uncertainties reported at the 95% confidence level.

obtained for each proton from eq 3 and the data illustrated in Figures 1 and 2. The paramagnetic relaxation rates, $1/T_{1p}$, for each oligonucleotide proton examined were found to vary linearly with the metal/duplex ratio. As can be seen in the tables, in all of the titrations, the relaxation rate of the AH2 proton is enhanced by approximately a factor of 10 over the rate of the next aromatic proton, if the G1H8 proton at the end of the helix is not considered. The rate of AH2 relaxation for Λ-$Ni(phen)_3^{2+}$ is 1.7 times greater than that of the Δ-enantiomer, and for the chromium complex, the rate in the presence of the Λ-enantiomer is enhanced by a factor of 2.4 over that of the Δ-isomer.

When the Λ-enantiomers are bound to the oligonucleotides, the order of relaxation rates for the aromatic protons are the same for both metals if end effects are neglected: AH2 followed by AH8, G3H8, and TMe. [In the case of $Cr(phen)_3^{3+}$, the G3H8 and TMe protons relax at the same rate within experimental uncertainty.] The similarity in the relaxation rate order is not apparent for the Δ-enantiomers because, with the exception of AH2, the relaxation rates measured for all protons when the chromium complex is bound are identical within experimental uncertainty.

The relaxation rates of the aromatic protons when the Λ-enantiomer is associated with the oligonucleotide are generally greater or equal to the rates observed in the presence of the Δ-enantiomer. The G3H8 proton, however, experiences faster relaxation when the Δ-isomer is bound. This is evident in Table I where $1/T_{1M}$ is found to be 62 s^{-1} with Δ-$Ni(phen)_3^{2+}$ and only 39 s^{-1} for the Λ-isomer. This observation is of some interest since G3H8 resides in the major groove of the DNA helix. Thus while broadening of the minor groove proton AH2 shows an enantioselectivity for the Λ-isomer, here the enantioselectivity in broadening a proton residing in the major groove favors the Δ-isomer.

Distance Calculations. Distances were calculated from the relaxation rates of the 1:1 complex, $1/T_{1M}$, as given in eq 1. The largest actual ratios for the chromium and nickel complex are 1 metal complex per 50 duplex oligonucleotides and 1 metal per 22 duplex oligonucleotides, respectively. At these ratios, greater than 98% of the complex is bound to $d(GTGCAC)_2$ on the basis of equilibrium binding data, and it is reasonable to assume that there will be no more than one complex bound per duplex oligonucleotide. Therefore, the stoichiometry of the complex, q, is assumed to be 1 at the ratios of metal complex to DNA used here. Tables I and II give the calculated values for $1/T_{1M}$ for the metal complexes associated with $d(GTGCAC)_2$.

The correlation time, τ_c, for each complex associated with oligonucleotide $d(GTGCAC)_2$ was evaluated by measuring the frequency dependence of $1/T_{1M}$. Relaxation measurements were carried out at 300 and 400 MHz, and the frequency-dependent part of eq 1, $f(\tau_c)$, was used to calculate the τ_c values. The τ_c values obtained by this method fall between 0.1 and 1 ns. Correlation times in this range maximize the value of $f(\tau_c)$ at 400 MHz and give the longest distances that could be obtained from the relaxation data. Therefore, the distances calculated with these experimental τ_c values may be regarded as upper limits.

For the purpose of these calculations, we have set $g(Cr(phen)_3^{3+}) = 2.0$ and $g(Ni(phen)_3^{2+}) = 2.2$. The chromium value is supported by the literature value of 1.984 for $Cr(bipy)_3^{3+}$ (Hauser et al., 1987). ESR spectra for tris(phenanthroline)nickel(II) or tris(bipyridine)nickel(II) have not been observed, but Ni(II) complexes generally display g values between 2 and 2.3; experimental g values for $Ni(H_2O)_6^{2+}$ and $Ni(NH_3)_6^{2+}$ are 2.25 (Hoskins et al., 1959) and 2.16 (Pate, 1960), respectively.

By use of these parameters, the distances between specific protons and the metal center may be calculated according to eq 1, and values obtained are given in Tables I and II. Note that the interatomic distances calculated for Λ- and Δ-$Ni(phen)_3^{2+}$ are uniformly shorter than those obtained with the chromium enantiomers. This observation may be explained by electron delocalization between the ligands and metal ion in the nickel complex (vide infra). On the basis of these calculations, the Λ-enantiomer appears closer to the protons in the minor groove of the oligonucleotide (AH2, AH1′, and C4H1′) than does the Δ-isomer in the case of both di- and trivalent metal complexes. The distances between the metal center and the major groove protons TMe, G3H8, and C4H5 are similar (within experimental error) for the Λ- and Δ-isomers. In the presence of $Ni(phen)_3^{2+}$, however, the G3H8 proton is closer to the metal center when the Δ-enantiomer is bound to the oligonucleotide.

Correlation of Distances with Structural Models. Structural models were designed to reflect binding orientations that could potentially be adopted by tris(phenanthroline) metal complexes bound to $d(GTGCAC)_2$. The distances derived from these models were compared with experimental distances. This analysis provides insight regarding the extent to which different binding modes may contribute to the overall interaction of the metal complex with the oligonucleotide.

A set of nine models was constructed, reflecting five different orientations of the metal complex intercalated in the major groove of B-form $d(GTGCAC)_2$ and four orientations where the Λ-enantiomer is surface bound in the major or minor groove. The intercalative models included three orientations where the complex is bound in the center and to the left and right side of the T·A base pair and two orientations where the complex is intercalated in the central 5′-GpC-3′ base pair step. The four surface-binding models have the Λ-enantiomer associated near the ApT base pair and near the central CpG base pair in the minor and major grooves of the DNA helix.

All of the models were energy minimized with the AMBER force field (Weiner et al., 1984, 1986) to ensure that all of the distances between atoms reflect reasonable van der Waals distances. For the intercalative orientations the starting oligonucleotide structure incorporated an open set of base pairs adapted from the crystal structure of proflavin intercalated into UpG·CpA (Aggarwal et al., 1984). While little perturbation of the initial B-DNA helix is required to accommodate the metal complex intercalated or surface bound in the major groove, surface binding in the minor groove requires that the DNA groove be widened slightly.

The intermolecular distances obtained from these models were converted to relaxation rates with eq 1 and combined in

Table III: Correlation of Structural Models of Tris(phenanthroline) Metal Complexes Bound to d(GTGCAC)$_2$

complex	correlation coeff[a]	% contribution of model		
		SB.AT[b]	INT.TGL[c]	INT.GCC[d]
Δ-Ni(phen)$_3^{2+}$	0.76	85	2	13
Λ-Ni(phen)$_3^{2+}$	0.91	94	2	4
Δ-Cr(phen)$_3^{3+}$	0.64	80	18	2
Λ-Cr(phen)$_3^{3+}$	0.84	93	4	3

[a] Correlation between the distances calculated on the basis of the relaxation data and the distances determined from a linear combination of structural models. Since the calculated distances for the nickel complexes were unreasonably short on the basis of van der Waals considerations, these values were increased for the purposes of modeling the complex on the oligonucleotide. The adjustment was carried out by multiplying the relation rates of all of the protons by a constant factor based on a structurally reasonable value for the AH2 proton. [b] SB.AT, Λ-isomer surface bound at the ApT base pair. [c] INT.TGL, metal complex intercalated toward the left side between the TpA and GpC base pairs. [d] INT.GCC, metal complex intercalated in the center between the GpC base pairs.

a linear fashion until the maximum correlation was obtained between the theoretical and experimental distances (Table III). It should be noted that in all cases distances calculated have been taken as internuclear distances between the protons under consideration and the metal center. To a first approximation, this assumes that the paramagnetism is confined to the metal ion. Also, as a result, distance differences with bound enantiomers result only from different binding interactions of the isomers with the helical structure and are not dependent upon the different distances present between any other atoms on the complex and the oligonucleotide in the diastereomer. For all of the complexes studied, the correlation coefficients were optimized by a linear combination of three of the nine models considered: (i) surface binding near the A·T base pair in the minor groove, (ii) intercalation in the major groove between the central base pairs, and (iii) intercalation to the left side between the T·A and G·C base pairs. Of these models, the major contribution that gives the best fit to the data is a minor groove surface-bound orientation. Our model for this interaction is illustrated in Figure 3.

The surface-binding model by itself, however, does not provide the best correlation with the experimental distances because the experimental distances between protons in the major groove and the metal center are shorter than those that would be predicted on the basis of a model where all of the complex was bound in the minor groove of the DNA. Adding small contributions for the major groove intercalative models improves the correlation coefficients considerably. For the Λ-enantiomers, the best fit of the experimental data is obtained when surface-binding model accounts for between 93% and 94% of the data and the intercalative model for 6%–7%. Comparison of the models with the experimental distances is shown in Figure 4. The results for Δ-enantiomers both correlate best with models that incorporate more of the major groove intercalative mode (between 15% and 20%), while maintaining a major contribution from the minor groove surface association. Poor overall correlation is nonetheless evident for the Δ-enantiomer binding models.

Limitations in the Model. This analysis was simplified by the use of a static oligonucleotide model with the metal complex positioned with average interproton distances. Consequently, potential errors resulting from differential mobility of oligonucleotide protons were not considered. The fact that certain protons have more degrees of freedom may have enhanced the broadening effectiveness of the paramagnetic complex causing the calculated average distances to be shorter than they actually are.

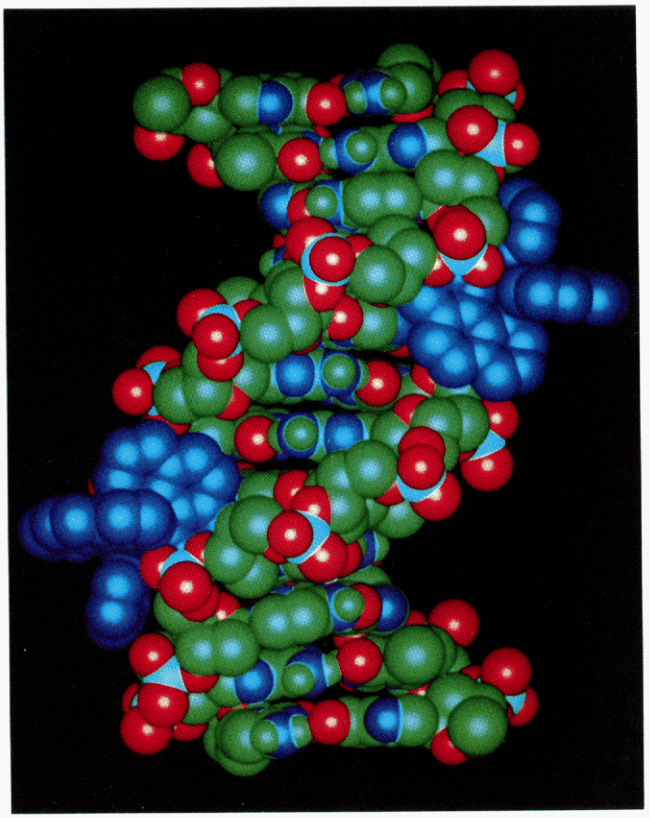

FIGURE 3: Model for the Λ-isomer of a tris(phenanthroline) metal complex (shown in blue) bound to DNA in the surface-bound mode in the minor groove.

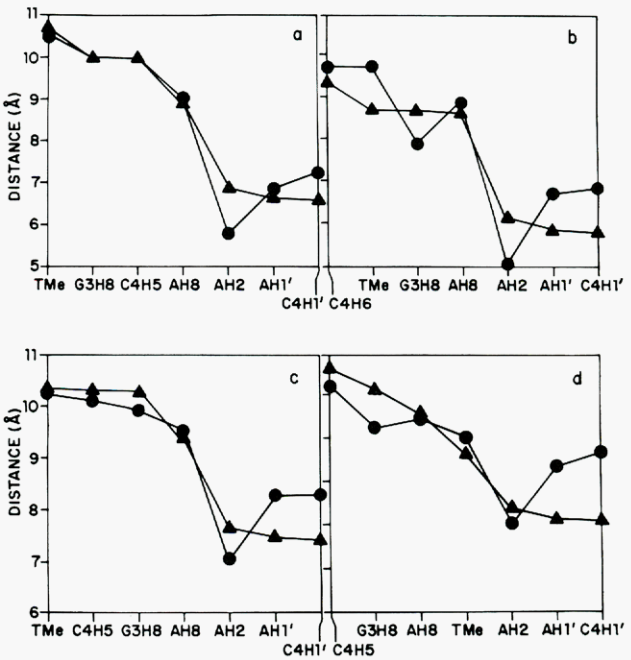

FIGURE 4: Comparison of calculated (▲) and experimental (●) metal–proton distances for Δ- (a) and Λ- (b) Ni(phen)$_3^{2+}$ and Δ- (c) and Λ- (d) Cr(phen)$_3^{3+}$.

The distances obtained from relaxation experiments using Ni(phen)$_3^{2+}$ are also much shorter than those that would be anticipated on the basis of molecular models. The extra enhancement in the relaxation of the DNA protons in the presence of the nickel complex may be attributed to electron spin-transfer mechanisms, which impart a partial radical character to the ligand. These mechanisms have been studied by measuring the isotropic chemical shifts of the ligand protons

in tris(1,10-phenanthroline)nickel(II) and tris(bipyridine)-nickel(II) complexes (Huang & Brewer, 1981; LaMar & Van Hecke, 1970; Wicholas & Drago, 1968; Wicholas, 1971). Since these nickel complexes are isotropic in the $^3A_{2g}$ ground state, dipolar contributions to the chemical shifts are negligible. The observed shifts are the result of a Fermi contact interaction generated by electron density at the proton nucleus (LaMar et al., 1973). Unpaired electron spin density on the ligand can arise from electron transfer in two directions: electrons can be donated from the ligand to the metal via a σ-delocalization mechanism resulting in a ligand cation radical, or alternatively, electron density could be back-donated from the $d\pi$ metal orbitals to the π^*-bonding orbitals of the ligand. Spin density on the ligand has been investigated by correlating NMR shift data with relative hyperfine coupling constants derived from INDO calculations for nickel bipyridine complexes (Huang & Brewer, 1981; Scarlet et al., 1970). The results of these studies indicate that σ-electron density transfer is the predominant mechanism operating in these complexes. Other studies have shown that *o*-phenanthroline complexes are similar to bipyridine complexes in this respect (Wicholas, 1971). Since ligand to metal electron transfer in $Ni(phen)_3^{2+}$ complexes generates unpaired electron density closer to the oligonucleotide in the $Ni(phen)_3^{2+}$–$d(GTGCAC)_2$ complex, enhanced paramagnetic relaxation via dipolar mechanisms might be expected for the oligonucleotide protons.

More efficient relaxation will result in shorter calculated distances for the nickel complex, but the relative order of the interatomic distances will be unaffected. Therefore, in order to better correlate the experimental data with the model, the experimental distances were normalized to reflect reasonable intermolecular distances based on the van der Waals radii of the oligonucleotide and the metal complex (see footnote to Table III).

Binding Modes of the Complexes to DNA. Earlier work has shown that $Ru(phen)_3^{2+}$ binds to DNA via two distinct modes; intercalation and surface binding (Barton et al., 1986). Both modes show a chiral preference, with the Δ-enantiomer favoring the intercalative orientation and the Λ-enantiomer preferring the surface-bound mode. The enantioselectivity associated with each binding mode is consistent with models where both isomers bind in the groove of the DNA with two of the *o*-phenanthroline ligands aligned along the groove of the DNA helix. For an intercalative interaction, one ligand is inserted between the base pairs, and the nonintercalated ligands align along the right-handed groove only for the Δ-isomer. For the Λ-isomer, one ligand must protrude outward to align the remaining two against the groove, and this we describe as the surface-bound interaction. The enantioselectivities associated with each binding interaction are not large in the case of phenanthroline complexes. The paramagnetic relaxation experiments conducted here are consistent with these binding models. Furthermore, the results here indicate that the surface-bound complex resides in the minor groove of the helix. The data obtained here cannot, however, be fully accommodated by interactions solely in the minor groove. Instead, the relative ordering of distances requires some contribution (moderate for Δ-isomers and low for Λ-isomers) of a major groove binding mode. The results then are, in addition, consistent with the other binding mode, intercalation, which favors the Δ-isomer and the lower positively charged species, residing in the major groove.

The relaxation data appear to weight the surface-bound interaction over the intercalative interaction. The reason why these data are more sensitive to contributions from the surface-bound mode is unclear. Differences in binding of these metal complexes to oligonucleotides as compared to polynucleotides have been found (Rehmann & Barton, 1990). Luminescence enhancement and single photon counting experiments for $Ru(phen)_3^{2+}$ bound to $d(GTGCAC)_2$ do indicate that tris(phenanthroline) metal complexes use similar binding modes when associating with the oligonucleotide and with calf thymus DNA (Rehmann & Barton, 1990), and the enhanced luminescence and presence of a long-lived component in the biphasic emission decay curves provide evidence that some of the complex is bound intercalatively. The short-lived luminescence component, which represents a mixture of the surface-bound species plus the metal complex free in solution, accounts for a larger proportion of the total binding to the oligonucleotide than it does with calf thymus DNA, however. Perhaps the fact that a 5′-pyr-pur-3′ step does not reside in the center of our short duplex also bears consideration. Also it appears that the results described here may give greater weight to short-range interactions (even requiring corrections to normalize distances at increased values). This may be seen also in the high sensitivity of the AH2 proton itself to broadening. In the surface-bound form, the metal center would reside closer to the helix than for the intercalative mode, and hence, greater weighting of this shorter distance interaction may occur.

The fact that the surface-bound mode provides the major contribution to the relaxation results does permit a reliable modeling of this minor groove surface-binding mode but little information with regard to models for the intercalative mode. Our model for this surface-bound interaction is given in Figure 3. In this model two phenanthroline ligands are seen to lie along the helical groove, in fact fitting quite closely within the helical channel, presumably maximizing hydrophobic and van der Waals interactions. Best correlation is obtained with the complex bound so that the metal is centered at the AT site. This correlation is consistent with the AT preference found to be associated with this mode (Barton et al., 1986) and perhaps reflects an increase in groove width and/or some electrostatic component associated with binding at this site. The model also reflects a clear enantioselectivity for the Λ-isomer in this binding mode, perhaps even to a greater extent than binding results would indicate. Actually for the Λ-enantiomers, all of the models predict similar distances for the minor groove protons AH2, AH1′, and C4H1′. Yet the distances, determined on the basis of the relaxation data, indicate that the AH2 proton is significantly closer to the metal complex than are the anomeric protons. This may be an indication that the dimensions of the minor groove deviate from the model, with the actual solution structure perhaps having a wider minor groove. Interestingly, from modeling, both isomers are easily accommodated in the major groove in a surface-bound interaction, but *the data clearly indicate that the surface binding is favored in the minor groove despite the relative sizes of grooves and complexes.* Large structural perturbations are actually required to model the Δ-isomer bound in the minor groove of B-DNA in any fashion, and in fact, a surface-bound model energy minimized for the Λ-enantiomer rather than for the Δ-enantiomer was used to fit the data. As a result, as well as presumably owing to our limited contribution of a well-defined intercalative model, the correlation coefficients are found to be significantly lower for the Δ-enantiomers compared to Λ-enantiomers; the data obtained in this experiment do not provide sufficient information to indicate how an appropriate model could be devised for this binding mode.

This minor groove surface-bound interaction is reminiscient of a common type of noncovalent association adopted by other cationic ligands that groove bind to DNA (Neidle et al., 1987). The polypyrroles netropsin (Patel & Shapiro, 1986) and distamycin (Klevit et al., 1986) and metalloporphyrin complexes (Ward et al., 1986) all surface bind in the minor groove of B-DNA with an AT preference. Although the mode of binding is unknown, the related complex bis(1,10-phenanthroline)copper(I) also associates with DNA in the minor groove (Kuwabara et al., 1986; Veal & Rill, 1988). The driving force for binding has been described as a combination of van der Waals and hydrophobic interactions with the surface of the minor groove and electrostatic interactions between the cationic complexes and the negatively charged phosphate backbone (Neidle et al., 1987). In the case of the polypyrroles netropsin and distamycin, hydrogen-bonding is also considered to be important. The tris(phenanthroline) metal complexes contain neither hydrogen-bonding donors nor acceptors. Nonetheless, this surface-bound mode is likely to be quite comparable to those for these groove-bound species and probably is based upon the same types of interactions. The association of molecules with a DNA helix either in the major or minor groove appears, then, to be determined not simply by considerations of accessibility but also by electrostatic and van der Waals factors.

Clearly there are many other potential models that may reflect important DNA binding orientations for these metal complexes. For example, surface binding is not constrained to occur at any particular orientation with respect to the base pairs of the oligonucleotide. Several more orientations could be considered. Also, the contribution from binding at the ends of the oligonucleotide, an interaction that is likely to occur for the chromium complexes, has not been addressed. Finally, modeling the oligonucleotide in the B conformation may not reflect its actual solution structure. The structure of the oligonucleotide in solution may accommodate orientations of the metal complex that the B form does not. The use of this set of models, however, does provide a profile for the binding of tris(phenanthroline) metal complexes that is consistent with the experimental data.

Conclusions. The substitution of paramagnetic centers into the DNA-binding transition metal complexes provides a facile and sensitive method to obtain structural information regarding the weak, noncovalent interactions of the complexes with the nucleic acid. Selective paramagnetic broadening of oligonucleotide protons by the metal complexes is observed, with differences evident as a function of metal chirality and charge. Paramagnetic broadening results with Λ-Ni(phen)$_3^{2+}$ and Λ-Cr(phen)$_3^{3+}$, which favor a surface-binding mode, indicate the preferential association of the complexes in the minor groove of the oligomer. From these results we conclude that the surface-binding interaction of tris(phenanthroline) complexes occurs in the minor groove of a DNA helix, and a model for this interaction is presented which correlates well with the relaxation data obtained. This surface-bound interaction appears comparable to other groove-binding models of small molecules on DNA, despite the fact that the tris(phenanthroline) complexes contain no hydrogen-bonding groups. The surface-bound model cannot, however, fully account for the relaxation data, especially for Δ-isomers, and a moderate contribution from major groove intercalactive binding is required. The smaller contribution to the relaxation data from this binding mode, however, makes it difficult to elucidate specific structural details associated with the interaction. The two binding models used in the analysis, with groove and enantiomeric preference, however, are consistent with the data and may provide a viable description of the association of tris(1,10-phenanthroline) metal complexes with the oligonucleotide d(GTGCAC)$_2$.

Acknowledgments

We thank Dr. Christopher Turner for his expert technical assistance in these experiments.

References

Aggarwal, A., Islam, S. A., Kuroda, R., & Neidle, S. (1984) *Biopolymers 23*, 1025–1041.
Barton, J. K. (1986) *Science 233*, 727–734.
Barton, J. K., Danishefsky, A., & Goldberg, J. (1984) *J. Am. Chem. Soc. 106*, 2172–2176.
Barton, J. K., Goldberg, J., Kumar, C. V., & Turro, N. J. (1986) *J. Am. Chem. Soc. 108*, 2018–2088.
Bloembergen, N., & Morgan, L. O. (1961) *J. Chem. Phys. 34*, 834.
Davies, N. R., & Dwyer, F. P. (1953) *Trans. Faraday Soc. 49*, 180–184.
Hauser, A., Mader, M., Robinson, W. T., Murugesen, R., & Ferguson, J. (1987) *Inorg. Chem. 26*, 1331.
Hein, F., & Herzog, S. (1965) in *Handbook of Preparative Inorganic Chemistry*, 2nd ed. (Brauer, G., Ed.) Vol. 2, p 1365, Academic Press, New York.
Herzog, S. (1956) *Chem. Tech. (Leipzig) 8*, 544.
Hoskins, R. H., Pastor, R. C., & Trigger, K. R. (1959) *J. Chem. Phys. 30*, 601.
Huang, T., & Brewer, D. (1981) *Can. J. Chem. 59*, 1689.
Kane-Maguire, N. A. P., & Hallock, J. S. (1979) *Inorg. Chim. Acta 35*, L309.
Kauffman, G. B., & Takahashi, L. T. (1966) *Inorg. Synth. 8*, 228.
Klevit, R. E., Wemmer, D. E., & Reid, B. R. (1986) *Biochemistry 25*, 3296.
Kumar, C. V., Barton, J. K., & Turro, N. J. (1985) *J. Am. Chem. Soc. 107*, 5518.
Kuwabara, M., Yoon, C., Goyne, T., Thederahn, T., & Sigman, D. (1986) *Biochemistry 25*, 7401.
LaMar, G., & van Hecke, G. (1970) *Inorg. Chem. 9*, 1546.
LaMar, G., Horrocks, W. DeW., & Holm, R. (1973) in *NMR of Paramagnetic Molecules*, Chapter 4, Academic Press, New York.
Lee, C. S., & Gorton, E. M., Neumann, H. M., & Hunt, H. R. (1966) *Inorg. Chem. 5*, 1397.
Mason, S. F., & Peart, B. J. (1973) *J. Chem. Soc., Dalton Trans.*, 949.
Mildvan, A. S., & Gupta, R. K. (1978) *Methods Enzymol. 49*, 322.
Neidle, S., Pearl, L., & Skelley, J. (1987) *Biochem. J. 243*, 1–13.
Pate, M. (1960) *J. Phys. Soc. Jpn. 15*, 2115.
Patel, D. J., & Shapiro, L. (1986) *J. Biol. Chem. 261*, 1230.
Rehmann, J. P., & Barton, J. K. (1990) *Biochemistry* (preceding paper in this issue).
Scarlet, M., Casey, A., & Craig, R. (1970) *Aust. J. Chem. 23*, 1333.
Scheek, R. M., Russo, N., Boelens, R., Kaptein, R., & van Boom, J. H. (1983) *J. Am. Chem. Soc. 105*, 2914.
Solomon, I. (1955) *Phys. Rev. 99*, 559.
Tran-Dinh S., Neumann, J., Huynh-dinh, T., Genissel, B., Igolen, J., & Simonnot, G. (1982) *Eur. J. Chem. 124*, 415–425.
Veal, J. M., & Rill, R. L. (1988) *Biochemistry 27*, 1822.

Ward, B., Skorobogty, A., & Dabrowiak, J. C. (1986) *Biochemistry 25*, 7827.
Weiner, S. J., Kollman, P. A., Case, D. A., Singh, U. C., Ghio, C., Alagona, G., Proteta, S., & Weiner, P. (1984) *J. Am. Chem. Soc. 106*, 765.
Weiner, S. J., Kollman, P. A., Nguyen, D. T., & Case, D. A. (1986) *J. Comp. Chem. 7*, 230.
Wicholas, M. (1971) *Inorg. Chem. 10*, 1086.
Wicholas, M., & Drago, R. (1968) *J. Am. Chem. Soc. 90*, 6946.

Deuterium Relaxation and Internal Motion in Solid Li-DNA†

Rolf Brandes,‡ Regitze R. Vold,* D. R. Kearns, and Allan Rupprecht§
Department of Chemistry, University of California—San Diego, La Jolla, California 92093
Received May 23, 1989; Revised Manuscript Received October 5, 1989

ABSTRACT: As part of an effort to explore the nature of the internal motion in solid polynucleotides, the spectral densities of motion $J_1(\omega_0)$ and $J_2(2\omega_0)$ have been measured for oriented, partially hydrated samples of calf thymus Li-DNA deuterated in the guanine and adenine 8-positions. Both spectral densities increase with increasing hydration level, J_1 is found to be 2–5 times larger than J_2, and their frequency dependence appears to be ω^{-1} and $\omega^{-3/2}$, respectively. The large values of the ratio J_1/J_2 rule out any in-plane torsional motion as the dominant relaxation mechanism in these samples, but a drop in this ratio at high hydration levels (G13 H_2O/nucleotide) may indicate increasing contributions from such torsional motion. Although a satisfactory fit to a particular motional model has yet to be achieved, our findings show that the librational motion of the C_8–D bond at or below a hydration level of 10 H_2O/nucleotide is approximately uniaxial, with correlation times for the motion in the range 0.2–3.0 μs.

Dry DNA is very hygroscopic. It readily absorbs water from the atmosphere unit, and at 94–98% relative humidity, originally lyophilized DNA has the appearance of a viscous liquid. The absorption of water is accompanied by internal and/or overall motion of larger and larger amplitude, until in solution the DNA is free to reorient completely.

While numerous techniques exist for studying the dynamics of DNA in solution, magnetic resonance techniques are uniquely suited for determination of molecular motion in the solid state. Several NMR studies have been performed on solid polynucleotides (Shindo et al., 1980, 1985, 1987; DiVerdi & Opella, 1981; Nall et al., 1981; Opella et al., 1981; Bendel et al., 1983; Mai et al., 1983; Fujiwara & Shindo, 1985; Brandes et al., 1986, 1988a,b; Vold et al., 1986) and, recently, on solid oligonucleotides (Kintanar et al., 1989) with the objective of characterizing the modes of motion responsible for NMR line shapes and spin–lattice relaxation behavior. It is by now well documented that NMR spin–lattic relaxation times drop precipitously as water is adsorbed and that this more efficient relaxation is caused by librational motion of increasing amplitude. At high humidity slower, large-angle motion takes place that has profound effects on the NMR spectra. This information has chiefly been obtained by analysis of phosphorus and deuterium line shapes and relaxation rates. Phosphorus NMR has given information about backbone motion while the deuterium work, relying on deuterium labeling of the purines, has reported on the mobility of the bases. Previous deuterium NMR studies of oriented samples of Li-DNA (Vold et al., 1986; Brandes et al., 1988b) have demonstrated that the purine C_8–D bonds are oriented approximately perpendicular to the helix axis and that a hydration levels of less than ca. 13 molecules of water per nucleotide the motion is nearly uniaxial with an amplitude of less than 15°. At higher hydration levels large-angle motion seems to occur predominantly in the plane of the base pairs (Shindo et al., 1987). This motion may ultimately lead to the damped torsional deformation modes generally assumed (Allison & Schurr, 1979; Barkley & Zimm, 1979; Allison et al., 1982; Schurr et al., 1989) to be responsible for strongly nonexponential fluorescence depolarization in solution.

In an earlier study (Brandes et al., 1986) we measured the spin–lattice relaxation times of hydrated powders of Na- and Li-DNA at 38.4 and 76.8 MHz and attempted an interpretation of the results in terms of a simple diffusion in a cone model. The frequency dependence of the observed relaxation rates (ω^{-1}) could not be reconciled with the cone model, which predicts the relaxation rate to be proportional to ω^{-2} in the range of rates of interest. It was concluded (Brandes et al., 1986) that the weaker frequency dependence might be associated with the predominance of collective modes of motion of unspecified origin, and the present study was undertaken in the hope of improving our understanding of such processes. Thus, we have measured the individual spectral densities of motion which characterize the spin–lattice relaxation behavior of DNA deuterons in samples of oriented calf thymus DNA. The new data rule out damped torsional oscillations (Allison et al., 1982) of the bases about the base normal as the principal cause of relaxation at hydration levels below ca. 13 H_2O/nucleotide. We have consequently analyzed the spectral density data in terms of a simple diffusion in a cone model (Wang & Pecora, 1980; Lipari & Szabo, 1981), a more general cone model that allows for two different rates of motion, and a model that combines diffusive wobble of the base normal with torsional deformation. None of these models can fully account for the observed relaxation behavior, but simple

† This work was supported by grants from the U.S. Public Health Service (GM35177), the Swedish Natural Research Council, and the Swedish Medical Science Research Council.
‡ Present address: Magnetic Resonance Unit 11-M, VA Medical Center, 4150 Clement St., San Francisco, CA 94121.
§ Permanent address: Arrhenius Laboratory, Division of Physical Chemistry, University of Stockholm, Stockholm, Sweden.

0006-2960/90/0429-1717$02.50/0 © 1990 American Chemical Society